THE JOURNAL OF PHYSICAL CHEMISTRY Letters

Letter

pubs.acs.org/JPCL

Molecular Orbital Rule for Quantum Interference in Weakly Coupled Dimers: Low-Energy Giant Conductivity Switching Induced by Orbital Level Crossing

Daijiro Nozaki,* Andreas Lücke, and Wolf Gero Schmidt

Lehrstuhl für Theoretische Materialphysik, Universität Paderborn, 33095 Paderborn, Germany

Supporting Information

ABSTRACT: Destructive quantum interference (QI) in molecular junctions has attracted much attention in recent years. It can tune the conductance of molecular devices dramatically, which implies numerous potential applications in thermoelectric and switching applications. There are several schemes that address and rationalize QI in single molecular devices. Dimers play a particular role in this respect because the QI signal may disappear, depending on the dislocation of monomers. We derive a simple rule that governs the occurrence of QI in weakly coupled dimer stacks of both alternant and nonalternant polyaromatic hydrocarbons (PAHs) and extends the Tada-Yoshizawa scheme. Starting from the Green's function formalism combined with the molecular orbital expansion approach, it is shown that QI-induced antiresonances and their energies can be predicted from the amplitudes of the respective monomer terminal molecular orbitals. The condition is illustrated for a toy model consisting of two hydrogen molecules and applied within density functional calculations to alternant dimers of oligo(phenylene-ethynylene) and nonalternant PAHs. Minimal dimer structure modifications that require only a few millielectronvolts and lead to an energy crossing of the essentially preserved monomer orbitals are shown to result in giant conductance switching ratios.

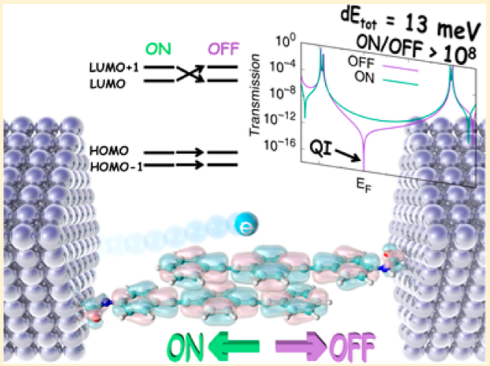

Charge transfer across noncovalently bonded molecular bridges is ubiquitous in nature, for example, in long-range signaling[1] or in photosynthesis,[2] but it also controls the functionality of man-made materials like organic semiconductors.[3,4] It depends sensitively on the distance and respective orientation of the molecules. Particularly pronounced conductance drops may result from so-called quantum interferences (QIs), that is, destructive superpositions of broadened electronic eigenstates.[5−10] This quantum effect on the molecular scale leads to a large on/off conductance ratio[11−23] that can be exploited in molecular switches and sensors.[24,25] It can also serve to filter hole or electron transmission and thus enhance the thermoelectric performance of molecular junctions.[26,27]

Many molecular junctions have been designed, and several theoretical models have been developed to understand the occurrence of quantum inferences. *Meta*-substituted phenyl rings,[12,18,20,22−37] T-shaped,[35−39] and cross-conjugated molecules[8,11,12,33,40] are intensively explored in this context. For instance, the Tada-Yoshizawa or molecular orbital (MO) approach can explain the QI at the center of HOMO−LUMO (H−L) gap by the cancellation of the contributions from frontier MOs.[10,15−23] The local molecular orbital (LMO) method allows for explaining the QI in cross-conjugated systems.[8,33,34,40]

Conductance measurements on dimer stacks[9,41−45] and theoretical studies on QI effect in π-stacked systems[9,22,45−47] have been performed to explore the influence of dislocations and rotations. Li et al. have reported the QI in covalently binded cyclophane dimers using the MO approach.[22] Solomon and coworkers[46,47] have shown that QI in tidily aligned stacks of alternant polyaromatic hydrocarbons (PAHs) can be understood in terms of the Coulson−Rushbrooke−McLachlan (CRM) pairing theorem.[48−51]

A general condition applicable to arbitrary dimer stacking configurations covering both alternant and nonalternant PAHs still needs to be established; however, the CRM theory cannot be applied to nonalternant PAHs, including odd-membered rings[50,51] such as azulene derivatives. Also, the applicability of the graphical Markussen−Stadler−Thygesen (MST) scheme and the MO approach has been under debate for some systems.[12,52−59] A detailed comparison of the predictions from the CRM theory, the MO approach, and the MST scheme for a variety of compounds and an analysis of their relationship to each other are summarized in ref 59.

The electron−hole symmetry frequently breaks in real molecules; that is, the Fermi energy does not coincide with the middle of the H−L gap. This happens, for example, if external fields are applied[50,60,61] or one of two monomers in

Received: December 20, 2016
Accepted: January 20, 2017
Published: January 20, 2017

DOI: 10.1021/acs.jpclett.6b02989
J. Phys. Chem. Lett. 2017, 8, 727−732

dimers is dislocated.[9,46,47] A scheme to predict the QI energy would be very helpful in such cases.

In this Letter, a condition for QI in weakly coupled molecular dimers is derived from the Green's function formalism.[62] We mention that a similar expression, starting from an MO expansion of the Green's function, was derived earlier.[15−23] The present scheme is first illustrated for the simple case of interacting H_2 molecules and then shown to correctly predict transmission antiresonances and their energies for dimers of both alternant and nonalternant PAHs. For this purpose, comparison is made to density functional theory (DFT)-based nonequilibrium Green's function (NEGF) and scattering approaches.

We start from the contacted molecular dimer Hamiltonian $H = H_M + \Sigma_L + \Sigma_R$, where H_M is the Hamiltonian for the dimer and $\Sigma_{L/R}$ are the self-energy terms for left/right contacts. The retarded/advanced Green's function is then given by $G^{r/a}(E) = [(E \pm i\delta)I - H_M - \Sigma_L - \Sigma_R]^{-1}$ and allows for calculating the transmission $T_{LR}(E) = \mathrm{Tr}[\Gamma_L G^r(E) \Gamma_R G^a(E)]$, where $\Gamma_{L/R}$ are the spectral densities of the left/right contacts defined as $\Gamma_{L/R} \equiv i[\Sigma_{L/R} - \Sigma^\dagger_{L/R}]$. Because the present focus is on the dimer QI, the contacts are treated in the wide-band limit (WBL) $\Sigma_{L/R} \equiv -i\gamma$. Also, we assume the coupling to the contacts to be sufficiently strong to rule out Coulomb blockades and allow for coherent tunneling. If ϕ_L (ϕ_R) are the atomic orbitals (AOs) that contact the dimer from the left (right) hand side, the electron transmission is

$$T_{LR}(E) = 4\gamma^2 |G^r_{LR}(E)|^2 \tag{1}$$

with the retarded Green's function in Lehmann representation[15−23,32,35,51]

$$G^r_{LR}(E) = \sum_m \frac{\langle \phi_L | \Psi_m \rangle \langle \Psi_m | \phi_R \rangle}{E + i\delta - \varepsilon_m} \tag{2}$$

Here Ψ_m is the m-th eigenvector of the contacted dimer obtained within WBL.

Let $\psi^{(L/R)}_{HO/LU}$ be the HOMO/LUMO of the isolated lhs/rhs monomers and $\varepsilon_{H/L}$ the corresponding energies. Upon coupling, the energy levels split, and the HOMO/HOMO−1 and LUMO/LUMO+1 energies are approximately given by $\varepsilon_H \pm \Delta_H$ and $\varepsilon_L \mp \Delta_L$, respectively. The splitting is small compared with the monomer's H−L gap $E_g = \varepsilon_L - \varepsilon_H \gg \Delta_{L/H}$, and the amplitudes of the monomer molecular orbitals are nearly preserved for sufficiently weak coupling. The frontier orbitals of the dimer stack (see also Figure 1a, left) can then be approximated by Brédas's MO expansion as[63]

$$\Psi_{LU+1} = (|\psi^{(L)}_{LU}\rangle \pm |\psi^{(R)}_{LU}\rangle)/\sqrt{2} \tag{3}$$

$$\Psi_{LU} = (|\psi^{(L)}_{LU}\rangle \mp |\psi^{(R)}_{LU}\rangle)/\sqrt{2} \tag{4}$$

$$\Psi_{HO} = (|\psi^{(L)}_{HO}\rangle \mp |\psi^{(R)}_{HO}\rangle)/\sqrt{2} \tag{5}$$

$$\Psi_{HO-1} = (|\psi^{(L)}_{HO}\rangle \pm |\psi^{(R)}_{HO}\rangle)/\sqrt{2} \tag{6}$$

Note that the molecular orbitals of the dimer stack are obtained here by linear combinations of the monomer MOs, in contrast with the LMO approach.[8,33,34] Assuming that the Green's function around the Fermi energy can be approximated from the four levels HOMO−1 to LUMO+1 and that the contributions from other states are negligible because of the large denominator in eq 2, one finds

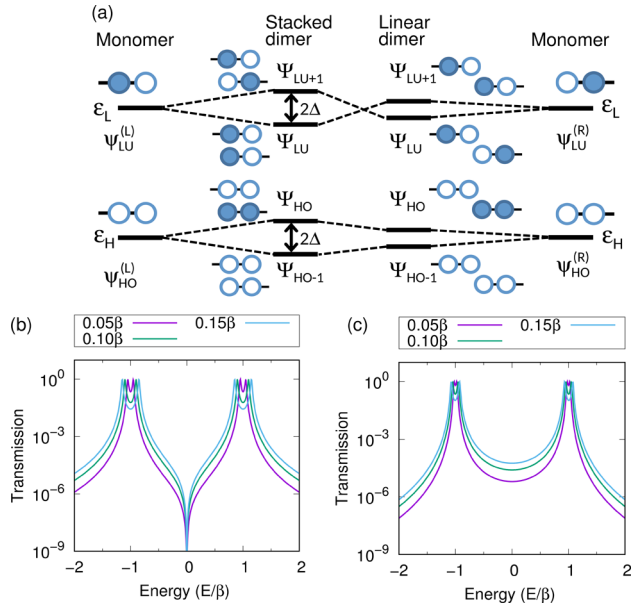

Figure 1. (a) MO diagram of weakly interacting H_2 molecules in stacked (left) and linear (right) configurations. (b) Transmission spectra of the stacked and (c) the linear dimer calculated within the WBL ($\Sigma_{L/R} = -i0.025|\beta|$) for different intermolecular couplings β (intramolecular transfer integral). The resonant peaks of the original monomers split at $E = \pm\beta$ due to the weak intermolecular interaction. Stronger intermolecular coupling leads to larger splitting. The QI is seen in stacked dimers as antiresonance in the middle of the gap.

$$G^r_{LR}(E) \approx \sum_{m=HO-1,HO,LU,LU+1} \frac{\langle \phi_L | \Psi_m \rangle \langle \Psi_m | \phi_R \rangle}{E - \varepsilon_m} \tag{7}$$

Here and in the following E contains a small imaginary part. The definitions of the MOs together with the relation

$$\langle \phi_L | \psi^{(R)}_{LU/HO} \rangle = \langle \phi_R | \psi^{(L)}_{LU/HO} \rangle = 0 \tag{8}$$

allow for expanding eq 7 as

$$2G^r_{LR}(E) \approx \pm\frac{a}{E - (\varepsilon_H - \Delta_H)} \mp \frac{a}{E - (\varepsilon_H + \Delta_H)} \mp \frac{b}{E - (\varepsilon_L - \Delta_L)} \pm \frac{b}{E - (\varepsilon_L + \Delta_L)} \tag{9}$$

with $a = \langle \phi_L | \psi^{(L)}_{HO} \rangle \langle \psi^{(R)}_{HO} | \phi_R \rangle$ and $b = \langle \phi_L | \psi^{(L)}_{LU} \rangle \langle \psi^{(R)}_{LU} | \phi_R \rangle$. Introducing a normalized energy in the H−L gap as $c = (E - \varepsilon_H)/E_g$, $0 \le c \le 1$, one finds

$$2G^r_{LR}(c) \approx \frac{\pm a}{cE_g + \Delta_H} \mp \frac{a}{cE_g - \Delta_H} \mp \frac{b}{(c-1)E_g + \Delta_L} \pm \frac{b}{(c-1)E_g - \Delta_L} \tag{10}$$

For midgap energies assuming $\Delta = \Delta_{L/R}$, one obtains

$$G^r_{LR}(c = 1/2) \approx \pm\frac{a - b}{E_g + 2\Delta} \mp \frac{a - b}{E_g - 2\Delta} \tag{11}$$

which yields the condition $a = b$ for midgap QI, that is

$$\langle \phi_L | \psi^{(L)}_{HO} \rangle \langle \psi^{(R)}_{HO} | \phi_R \rangle = \langle \phi_L | \psi^{(L)}_{LU} \rangle \langle \psi^{(R)}_{LU} | \phi_R \rangle \tag{12}$$

Using eqs 3−6 and 8, this can be written as

DOI: 10.1021/acs.jpclett.6b02989
J. Phys. Chem. Lett. 2017, 8, 727−732

$$\langle \phi_L|\Psi_{HO}\rangle\langle\Psi_{HO}|\phi_R\rangle = \langle \phi_L|\Psi_{LU}\rangle\langle\Psi_{LU}|\phi_R\rangle \quad (13)$$

Equation 13 allows for the prediction of midgap antiresonances from the signs and amplitudes of the dimer HOMO and LUMO at the left and right terminal contacts.

If eq 13 holds exactly, then QI occurs at the exact middle of the H−L gap, as predicted by the MO approach.[15−23] As long as eq 7 is valid, however, the antiresonance energy is obtained from the MO terminal amplitudes by

$$c = \frac{a \pm \sqrt{ab\Delta_r + (a - b\Delta_r)(a - b/\Delta_r)\delta_L^2}}{a - b\Delta_r};\ \delta_L = \frac{\Delta_L}{E_g},\ \Delta_r = \frac{\Delta_L}{\Delta_H} \quad (14)$$

This is seen from the expansion of eq 10 with respect to c by asserting $G^r_{LR}(c) = 0$. Note that the choice of parameters with $c = 1/2$ and $\Delta = \Delta_{L/R}$ in eq 14 corresponds to eq 13 and thus this leads to the Tada−Yoshizawa scheme.[15−23] The present approach, however, is more general and allows for predicting antiresonance energies within the H−L gap using eq 14.

Two weakly interacting hydrogen molecules, cf. Figure 1, are an illustrative toy system to visualize the condition derived here. Sliding the upper/lower H_2 monomer from the left/right-hand side to form a dimer, one immediately sees that relation 13 holds true for arbitrary stacked dimer AOs ϕ_L and ϕ_R but not for the linear configuration. Note that the unoccupied MO levels cross during the translocation because the LUMO+1 (LUMO) stabilizes (unstabilizes) due to the bonding (antibonding) orbital interactions. This level crossing invalidates relation 13 for the linear case. Thus one expects an antiresonance in the middle of the gap for the stacked configuration only. This is confirmed by the calculated transmission shown in Figure 1b,c: Only in the former is there an antiresonance in the middle of the gap. The resonances split due to the weak coupling of the molecules in both cases. The essential role of the level crossing for the electron transport will be investigated in more detail below for relevant complexes.

Let us turn to a more realistic system, dimers of oligo(phenylene-ethynylene) (OPE) connected to conducting carbon nanotubes (CNTs) via peptide linkers, cf. Figure 2a. The atomic structure of various dimer junctions with different CNT−CNT distances was determined using the density -functional tight-binding (DFTB+) method[64,65] with periodic boundary conditions (see Supporting Information (SI)). Thereafter, the electron transmission was calculated using the NEGF method,[66] as implemented in the DFTB+NEGF code.[67] The calculated transmission spectra and relevant monomer MOs for three different stacking configurations are shown in Figure 2b,d−f, respectively. It can be seen that all configurations show QI in the gap and slightly split eigenstates. This is in accordance with the molecular orbital rule (relation 13): The products $\langle \phi_L|\Psi_{HO}\rangle\langle\Psi_{HO}|\phi_R\rangle$ in Figure 2d−f are positive for d = 6.92 Å and negative for d = 0 and 13.83 Å and thus agree in sign with $\langle \phi_L|\Psi_{LU}\rangle\langle\Psi_{LU}|\phi_R\rangle$ for all corresponding models; see Figure 2d−f. These findings were corroborated by a completely parameter-free approach, that is, the direct solution of the scattering problem[68] based on the DFT electronic structure obtained from the plane-wave-based Quantum espresso package.[69] Thereby the PWcond module[70] was used. Technical details of the calculations were chosen similar to previous work by some of the present authors.[71] The frontier orbitals obtained with the Quantum espresso package (see SI) resemble closely the DFTB+ results in Figure 2d−f. In

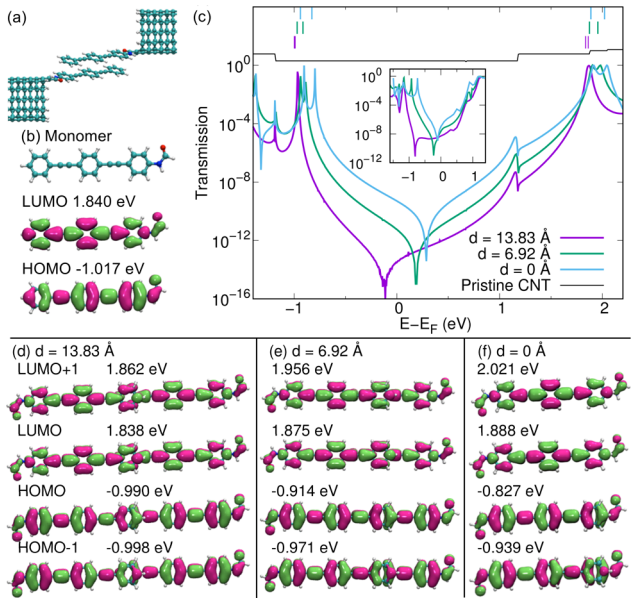

Figure 2. (a) Relaxed OPE dimer configuration (with dislocation d = 0 Å, cf. Figure 3c, magnified in Figure S2) connected to CNTs, (b) OPE monomer frontier MOs, and (c) electron transmission calculated for three dimer configurations with different d using the NEGF as well as first-principles scattering approach (inset). The spectral features at $E - E_F$ = 1.2 eV are related to the van Hove singularity of pristine CNTs. (d−f) Top views of the dimer MOs with respective eigenenergies. These energies are indicated in the upper part of the transmission diagram.

particular, they fulfill relation 13. Accordingly, also the transmission obtained using the scattering approach shows marked antiresonances in the midgap region for all three stacking configurations; see the inset of Figure 2c.

The influence of the relative dislocation distance d (cf. Figure 3c) on the OPE dimer transmission is explored by rigidly shifting the monomers with respect to each other (see also refs 9, 46, and 47). Those rigid monomers are separated by 3.53 Å. It can be seen that midgap antiresonances may be switched on and off by varying d, while the resonances barely shift in energy, cf. Figure 3. This is shown exemplarily by the blue and red lines and curves in Figure 3a,b, respectively. We mention that the CRM pairing theorem cannot be applied to the alternant OPEs with distance d = 4.25 Å (see SI Figure S4): The stacked dimer configuration forms an odd-membered loop between upper and lower monomers at this distance, which hampers application of the starring argument.[46−50] On the contrary, relation 13 correctly predicts a QI for this configuration (see Figure 3c,d). When d = 4.25 Å (5.59 Å), the product in $\langle \phi_L|\Psi_{HO}\rangle\langle\Psi_{HO}|\phi_R\rangle$ agrees (disagrees) in sign with $\langle \phi_L|\Psi_{LU}\rangle\langle\Psi_{LU}|\phi_R\rangle$, resulting in the appearance (absence) of antiresonance.

As exemplarily shown in the SI (Figures S8 and S9), the position of the antiresonance does not always coincide with the Fermi energy. The energy of the antiresonances from terminal MOs is approximately given by eq 14. In the case of the dimer in Figure 3c, for example, with $a = -1.64 \times 10^{-3}$, $b = -7.85 \times 10^{-3}$, $\delta_L = 1.53 \times 10^{-2}$, and $\Delta_r = 7.59 \times 10^{-1}$, one obtains c = 0.34 from eq 14, close to the exact value c = 0.32. Another notable feature in Figure 3a is the constant interval (∼2.5 Å at $E = E_F$) of the appearance of the QI w.r.t. dislocation, as already discussed in ref 9. This interval corresponds to twice the MO node separation in axial direction (also ∼2.5 Å in Figure 3b).

DOI: 10.1021/acs.jpclett.6b02989
J. Phys. Chem. Lett. 2017, 8, 727−732

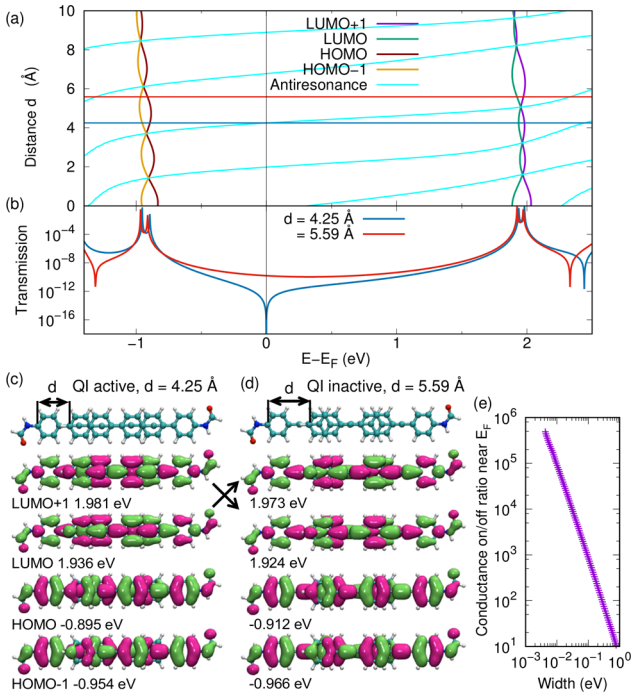

Figure 3. (a) Evolution of molecular energy levels and corresponding (anti)resonances in dependence on the dislocation *d*. (b) Calculated transmission spectra at the horizontal lines. Thereby featureless contacts attached to the terminal p_z orbitals with γ = 0.1 eV are assumed. (c,d) Frontier MOs of the dimers. The level crossing is indicated. (e) Dependence of the transmission on/off ratio on the energy width sampling around the Fermi energy.

The switching interval between QI and no QI regime can thus be related to the change of bonding/antibonding interaction between the lobes of the monomers' MOs; see, for example, Figure 1.

The variation of *d* between 4.25 and 5.59 Å affects the calculated total energy by 13 meV only but leads to a LUMO and LUMO+1 crossing, as indicated by arrows in Figure 3c,d. This, in turn, induces QI and leads to a giant on/off transmission ratio of up to 10^8 at the Fermi energy and in its vicinity, cf. Figure 3e. From the orbital energy crossings visualized in Figure 3a, one sees that further conductance switchings occur while varying *d*, for example, for *d* = 6.80 Å. The geometry-dependent level crossing thus allows us to modify the current by several orders of magnitude with minimal energy.

The molecular orbital rule derived here is not restricted to alternant PAHs. Results for nonalternant acephenanthrylene derivatives connected to conductive CNTs are shown in Figure 4a–d. The transmission calculated within the NEGF method shows a marked QI in the H-L gap for model 1. This is expected from the dimer's frontier MOs that satisfy relation 13, as can be seen from Figure 4e. This is not the case for model 2 (Figure 4f), again due to a level crossing: A slight shift by 0.47 Å accompanied by an energy increase of 30 meV quenches the QI. We mention that the MST scheme[12,52−54] is not applicable to the nonalternant PAH dimers in Figure 4 (cf. SI Figure S6) because the bonds between the monomers are not defined unambiguously.

Finally, we mention that the accuracy of the present approach depends obviously on the level of theory used for the underlying electronic structure calculations and can be

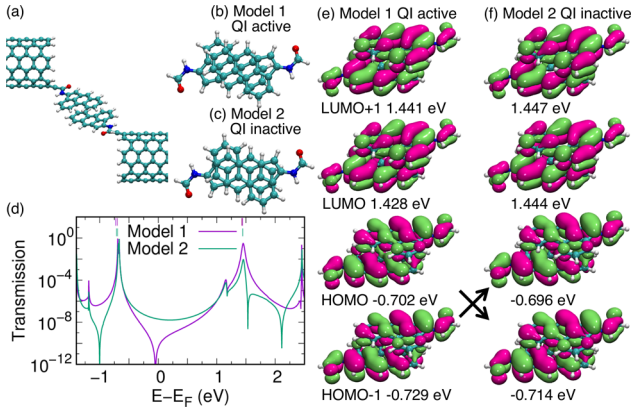

Figure 4. Relaxed nonalternant PAH dimers (see text) inside (a) and top views (b,c). (d) Transmission spectra and (e,f) frontier MOs of the truncated dimers with level crossing in occupied states. Their eigenenergies are indicated in panel d with vertical lines.

improved, for example, by including quasiparticle effects in the electronic self-energies: The same framework can then be used, but the eigenstates and eigenenergies $\{\varepsilon_i^{KS}, |\Psi_i^{KS}\}$ are to be replaced by the corresponding quasi-particle quantities $\{\varepsilon_i^{QP}, |\Psi_i^{QP}\}$.[72−79]

In summary, a general condition for the appearance of QIs in the electron transmission through weakly coupled dimers has been derived within the Green's function formalism combined with an MO expansion.[15−23] It is expected to assist in the design of molecular devices that exploit QI effects: The molecular orbital rule derived here allows for the reliable prediction of antiresonances and their energies from the terminal amplitudes of the frontier MOs. In particular, the on/off switching behavior of QI for specific dimer distances is traced to the level crossing of dimer MOs. This mechanism allows for controlling, switching, and tuning the conductance of essentially rigid molecular configurations with minimal displacements and energy; see Frisenda et al.[9]

■ ASSOCIATED CONTENT

Supporting Information

The Supporting Information is available free of charge on the ACS Publications website at DOI: 10.1021/acs.jpclett.6b02989.

Computational details of structure optimizations and transport calculations using DFTB+NEGF and Quantum espresso packages accompanied by corresponding atomic coordinates and application of the CRM pairing theorem, the MST diagrammatic approach, and TY approach to alternant and nonalternant dimer systems. (PDF)

■ AUTHOR INFORMATION

Corresponding Author

*E-mail: daijiro.nozaki@upb.de.

ORCID

Daijiro Nozaki: 0000-0002-1173-1648

Funding

No competing financial interests have been declared.

Notes

The authors declare no competing financial interest.

DOI: 10.1021/acs.jpclett.6b02989
J. Phys. Chem. Lett. 2017, 8, 727−732

■ ACKNOWLEDGMENTS

We gratefully acknowledge DFG financial support (FOR1700, FOR1405) and grants of high-performance computer time by the Paderborn Center for Parallel Computing (PC^2) and the HLRS Stuttgart.

■ REFERENCES

(1) Merino, E. J.; Boal, A. K.; Barton, J. K. Biological Contexts for DNA Charge Transport Chemistry. *Curr. Opin. Chem. Biol.* **2008**, *12*, 229−237.
(2) Brettel, K.; Leibl, W. Electron Transfer in Photosystem I. *Biochim. Biophys. Acta, Bioenerg.* **2001**, *1507*, 100−114.
(3) Coropceanu, V.; Cornil, J.; da Silva Filho, D. A.; Olivier, Y.; Silbey, R.; Brédas, J.-L. Charge Transport in Organic Semiconductors. *Chem. Rev.* **2007**, *107*, 926−952.
(4) Li, P.; Cui, Y.; Song, C.; Zhang, H. Electronic and Charge Transport Properties of Dimers of Dithienothiophenes: Effect of Structural Symmetry and Linking Mode. *RSC Adv.* **2015**, *5*, 50212.
(5) Aradhya, S. V.; Venkataraman, L. Single-molecule Junctions beyond Electronic Transport. *Nat. Nanotechnol.* **2013**, *8*, 399−410.
(6) Su, T. A.; Neupane, M.; Steigerwald, M. L.; Venkataraman, L.; Nuckolls, C. Chemical Principles of Single-Molecule Electronics. *Nat. Rev. Mater.* **2016**, *1*, 16002.
(7) Hong, W.; Valkenier, H.; Meszaros, G.; Manrique, D. Z.; Mishchenko, A.; Putz, A.; Garcia, P. M.; Lambert, C. J.; Hummelen, J. C.; Wandlowski, T. An MCBJ Case Study: The Influence of π-Conjugation on the Single-Molecule Conductance at a Solid/Liquid Interface. Beilstein. *Beilstein J. Nanotechnol.* **2011**, *2*, 699−713.
(8) Guédon, C. M.; Valkenier, H.; Markussen, T.; Thygesen, K. S.; Hummelen, J. C.; van der Molen, S. J. Observation of Quantum Interference in Molecular Charge Transport. *Nat. Nanotechnol.* **2012**, *7*, 305−309.
(9) Frisenda, R.; Janssen, V. A. E. C.; Grozema, F. C.; van der Zant, H. S. J.; Renaud, N. Mechanically Controlled Quantum Interference in Individual π-stacked Dimers. *Nat. Chem.* **2016**, *8*, 1099−1104.
(10) Ratner, M. A. Bridge-Assisted Electron Transfer: Effective Electronic Coupling. *J. Phys. Chem.* **1990**, *94*, 4877−4883.
(11) Darwish, N.; Diez-Perez, I.; Da Silva, P.; Tao, N.; Gooding, J. J.; Paddon-Row, M. N. Observation of Electrochemically Controlled Quantum Interference in a Single Anthraquinone-Based Norbornylogous Bridge Molecule. *Angew. Chem., Int. Ed.* **2012**, *51*, 3203−3206.
(12) Markussen, T.; Stadler, R.; Thygesen, K. S. The Relation between Structure and Quantum Interference in Single Molecule Junctions. *Nano Lett.* **2010**, *10*, 4260−4265.
(13) Baer, R.; Neuhauser, D. Phase Coherent Electronics: A Molecular Switch Based on Quantum Interference. *J. Am. Chem. Soc.* **2002**, *124*, 4200−4201.
(14) Emberly, E. G.; Kirczenow, G. Antiresonances in Molecular Wires. *J. Phys.: Condens. Matter* **1999**, *11*, 6911.
(15) Tada, T.; Yoshizawa, K. Quantum Transport Effects in Nanosized Graphite Sheets. *ChemPhysChem* **2002**, *3*, 1035−1037.
(16) Tada, T.; Yoshizawa, K. Quantum Transport Effects in Nanosized Graphite Sheets. II. Enhanced Transport Effects by Heteroatoms. *J. Phys. Chem. B* **2003**, *107*, 8789−8793.
(17) Yoshizawa, K.; Tada, T.; Staykov, A. Orbital Views of the Electron Transport in Molecular Devices. *J. Am. Chem. Soc.* **2008**, *130*, 9406−9413.
(18) Yoshizawa, K. An Orbital Rule for Electron Transport in Molecules. *Acc. Chem. Res.* **2012**, *45*, 1612−1621.
(19) Tsuji, Y.; Staykov, A.; Yoshizawa, K. Orbital Control of the Conductance Photoswitching in Diarylethene. *J. Phys. Chem. C* **2009**, *113*, 21477−21483.
(20) Tsuji, Y.; Staykov, A.; Yoshizawa, K. Orbital Views of Molecular Conductance Perturbed by Anchor Units. *J. Am. Chem. Soc.* **2011**, *133*, 5955−5965.
(21) Taniguchi, M.; Tsutsui, M.; Mogi, R.; Sugawara, T.; Tsuji, Y.; Yoshizawa, K.; Kawai, T. Dependence of Single-Molecule Conductance on Molecule Junction Symmetry. *J. Am. Chem. Soc.* **2011**, *133*, 11426−11429.
(22) Li, X.; Staykov, A.; Yoshizawa, K. Orbital Views on Electron Transport Properties of Cyclophanes: Insight into Intermolecular Transport. *Bull. Chem. Soc. Jpn.* **2012**, *85*, 181−188.
(23) Koga, J.; Tsuji, Y.; Yoshizawa, K. Orbital Control of Single-Molecule Conductance Perturbed by π-Accepting Anchor Groups: Cyanide and Isocyanide. *J. Phys. Chem. C* **2012**, *116*, 20607−20616.
(24) Cardamone, D. M.; Stafford, C. A.; Mazumdar, S. Controlling Quantum Transport through a Single Molecule. *Nano Lett.* **2006**, *6*, 2422−2426.
(25) Ke, S. H.; Yang, W. T.; Baranger, H. U. Quantum-Interference-Controlled Molecular Electronics. *Nano Lett.* **2008**, *8*, 3257−3261.
(26) Bergfield, J. P.; Stafford, C. A. Thermoelectric Signatures of Coherent Transport in Single-Molecule Heterojunctions. *Nano Lett.* **2009**, *9*, 3072−3076.
(27) Bergfield, J. P.; Solis, M. A.; Stafford, C. A. Giant Thermoelectric Effect from Transmission Supernodes. *ACS Nano* **2010**, *4*, 5314−5320.
(28) Sautet, P.; Joachim, C. Electronic Interference Produced by a Benzene Embedded in a Polyacetylene Chain. *Chem. Phys. Lett.* **1988**, *153*, 511−516.
(29) Walczak, K. The Role of Quantum Interference in Determining Transport Properties of Molecular Bridges. *Cent. Eur. J. Chem.* **2004**, *2*, 524−533.
(30) Stafford, C. A.; Cardamone, D. M.; Mazumdar, S. M. The Quantum Interference Effect Transistor. *Nanotechnology* **2007**, *18*, 424014.
(31) Donarini, A.; Begemann, G.; Grifoni, M. All-electric Spin Control in Interference Single Electron Transistors. *Nano Lett.* **2009**, *9*, 2897−2902.
(32) Hansen, T.; Solomon, G. C.; Andrews, D. Q.; Ratner, M. A. Interfering Pathways in Benzene: An analytical Treatment. *J. Chem. Phys.* **2009**, *131*, 194704.
(33) Markussen, T.; Schiötz, J.; Thygesen, K. S. Electrochemical Control of Quantum Interference in Anthraquinone-Based Molecular Switches. *J. Chem. Phys.* **2010**, *132*, 224104.
(34) Markussen, T.; Thygesen, K. S. Temperature Effects on Quantum Interference in Molecular Junctions. *Phys. Rev. B: Condens. Matter Mater. Phys.* **2014**, *89*, 085420.
(35) Solomon, G. C.; Andrews, D. Q.; Hansen, T.; Goldsmith, R. H.; Wasielewski, M. R.; Van Duyne, R. P.; Ratner, M. A. Understanding Quantum Interference in Coherent Molecular Conduction. *J. Chem. Phys.* **2008**, *129*, 054701.
(36) Lovey, D. A.; Romero, R. H. Quantum Interference through Gated Single-Molecule Junctions. *Chem. Phys. Lett.* **2012**, *530*, 86−92.
(37) Chen, S.; Zhang, Y.; Koo, S.; Tian, H.; Yam, C.; Chen, G.; Ratner, M. A. Interference and Molecular Transport—A Dynamical View: Time-Dependent Analysis of Disubstituted Benzenes. *J. Phys. Chem. Lett.* **2014**, *5*, 2748−2752.
(38) Papadopoulos, T. A.; Grace, I. M.; Lambert, C. J. Control of Electron Transport through Fano Resonances in Molecular Wires. *Phys. Rev. B: Condens. Matter Mater. Phys.* **2006**, *74*, 193306.
(39) Solomon, G. C.; Andrews, D. Q.; Van Duyne, R. P.; Ratner, M. A. When Things Are Not as They Seem: Quantum Interference Turns Molecular Electron Transfer "Rules" Upside Down. *J. Am. Chem. Soc.* **2008**, *130*, 7788−7789.
(40) Perrin, M. L.; Frisenda, R.; Koole, M.; Seldenthuis, J. S.; Gil, J. A. C.; Valkenier, H.; Hummelen, J. C.; Renaud, N.; Grozema, F. C.; Thijssen.; et al. Large Negative Differential Conductance in Single-molecule Break Junctions. *Nat. Nanotechnol.* **2014**, *9*, 830−834.
(41) Wu, S.; González, M. T.; Huber, R.; Grunder, S.; Mayor, M.; Schönenberger, C.; Calame, M. Molecular Junctions based on Aromatic Coupling. *Nat. Nanotechnol.* **2008**, *3*, 569−574.
(42) Li, C.; Stepanenko, V.; Lin, M.-J.; Hong, W.; Würthner, F.; Wandlowski, T. Charge Transport through Perylene Bisimide Molecular Junctions: An Electrochemical Approach. *Phys. Status Solidi B* **2013**, *250*, 2458−2467.

DOI: 10.1021/acs.jpclett.6b02989
J. Phys. Chem. Lett. 2017, 8, 727−732

(43) Frisenda, R.; van der Zant, H. S. J. Transition from Strong to Weak Electronic Coupling in a Single-Molecule Junction. *Phys. Rev. Lett.* **2016**, *117*, 126804.
(44) Schneebeli, S. T.; Kamenetska, M.; Cheng, Z.; Skouta, R.; Friesner, R. A.; Venkataraman, L.; Breslow, R. Single-Molecule Conductance through Multiple $\pi-\pi$-Stacked Benzene Rings Determined with Direct Electrode-to-Benzene Ring Connections. *J. Am. Chem. Soc.* **2011**, *133*, 2136−2139.
(45) Vázquez, H.; Skouta, R.; Schneebeli, S.; Kamenetska, M.; Breslow, R.; Venkataraman, L.; Hybertsen, M. S. Probing the Conductance Superposition Law in Single-molecule Circuits with Parallel Paths. *Nat. Nanotechnol.* **2012**, *7*, 663−667.
(46) Solomon, G. C.; Vura-Weis, J.; Herrmann, C.; Wasielewski, M. R.; Ratner, M. A. Understanding Coherent Transport through π-Stacked Systems upon Spatial Dislocation. *J. Phys. Chem. B* **2010**, *114*, 14735−14744.
(47) Li, Q.; Solomon, G. C. Exploring Coherent Transport through π-stacked Systems for Molecular Electronic Devices. *Faraday Discuss.* **2014**, *174*, 21−35.
(48) Coulson, C. A.; Rushbrooke, G. S. Note on the Method of Molecular Orbitals. *Math. Proc. Cambridge Philos. Soc.* **1940**, *36*, 193−200.
(49) McLachlan, A. D. The Pairing of Electronic States in Alternant Hydrocarbons. *Mol. Phys.* **1959**, *2*, 271−284.
(50) Pedersen, K. G. L.; Strange, M.; Leijnse, M.; Hedegård, P.; Solomon, G. C.; Paaske, J. Quantum Interference in Off-resonant Transport through Single Molecules. *Phys. Rev. B: Condens. Matter Mater. Phys.* **2014**, *90*, 125413.
(51) Strange, M.; Seldenthuis, J. S.; Verzijl, C. J. O.; Thijssen, J. M.; Solomon, G. C. Interference Enhanced Thermoelectricity in Quinoid Type Structures. *J. Chem. Phys.* **2015**, *142*, 084703.
(52) Markussen, T.; Stadler, R.; Thygesen, K. S. Graphical Prediction of Quantum Interference-induced Transmission Nodes in Functionalized Organic Molecules. *Phys. Chem. Chem. Phys.* **2011**, *13*, 14311−14317.
(53) Pedersen, K. G. L.; Borges, A.; Hedegård, P.; Solomon, G. C.; Strange, M. Illusory Connection between Cross-Conjugation and Quantum Interference. *J. Phys. Chem. C* **2015**, *119*, 26919−26924.
(54) Borges, A.; Fung, E.-D.; Ng, F.; Venkataraman, L.; Solomon, G. C. Probing the Conductance of the σ-System of Bipyridine Using Destructive Interference. *J. Phys. Chem. Lett.* **2016**, *7*, 4825−4829.
(55) Tsuji, Y.; Hoffmann, R. Frontier Orbital Control of Molecular Conductance and its Switching. *Angew. Chem., Int. Ed.* **2014**, *53*, 4093−4097.
(56) Xia, J.; Capozzi, B.; Wei, S.; Strange, M.; Batra, A.; Moreno, J. R.; Amir, R. J.; Amir, E.; Solomon, G. C.; Venkataraman, L.; et al. Breakdown of Interference Rules in Azulene, a Nonalternant Hydrocarbon. *Nano Lett.* **2014**, *14*, 2941−2945.
(57) Stadler, R. Comment on "Breakdown of Interference Rules in Azulene, a Nonalternant Hydrocarbon. *Nano Lett.* **2015**, *15*, 7175−7176.
(58) Strange, M.; Solomon, G. C.; Venkataraman, L.; Campos, L. M. Reply to "Comment on 'Breakdown of Interference Rules in Azulene, a Nonalternant Hydrocarbon'. *Nano Lett.* **2015**, *15*, 7177−7178.
(59) Zhao, X.; Geskin, V.; Stadler, R. Destructive Quantum Interference in Electron Transport: A Reconciliation of the Molecular Orbital and the Atomic Orbital Perspective. *J. Chem. Phys.* **2017**, *146*, 092308.
(60) Kubatkin, S.; Danilov, A.; Hjort, M.; Cornil, J.; Brédas, J.-L.; Stuhr-Hansen, N.; Hedegård, P.; Bjørnholm, T. Single-Electron Transistor of a Single Organic Molecule with Access to Several Redox States. *Nature* **2003**, *425*, 698−701.
(61) Koole, M.; Thijssen, J. M.; Valkenier, H.; Hummelen, J. C.; van der Zant, H. S. J. Electric-Field Control of Interfering Transport Pathways in a Single-Molecule Anthraquinone Transistor. *Nano Lett.* **2015**, *15*, 5569−5573.
(62) Datta, S. *Electronic Transport in Mesoscopic Systems*; Cambridge University Press: Cambridge, U.K., 1995.
(63) Brédas, J. L.; Calbert, J. P.; da Silva Filho, D. A.; Cornil, J. Organic Semiconductors: A Theoretical Characterization of the Basic Parameters Governing Charge Transport. *Proc. Natl. Acad. Sci. U. S. A.* **2002**, *99*, 5804−5809.
(64) Frauenheim, T.; Seifert, G.; Elsterner, M.; Hajnal, Z.; Jungnickel, G.; Porezag, F.; Suhai, S.; Scholz, R. A Self-Consistent Charge Density-Functional Based Tight-Binding Method for Predictive Materials Simulations in Physics, Chemistry and Biology. *Phys. Status Solidi B* **2000**, *217*, 41−62.
(65) Rauls, E.; Elsner, J.; Gutierrez, R.; Frauenheim, T. Stoichiometric and Non-stoichiometric $(10\bar{1}0)$ and $(11\bar{2}0)$ Surfaces in 2H−SiC: A Theoretical Study. *Solid State Commun.* **1999**, *111*, 459−464.
(66) Nozaki, D.; Toher, C.; Cuniberti, G. Low-Energy Conformational Gating in π-Conjugated Molecular Junctions. *J. Phys. Chem. Lett.* **2013**, *4*, 4192−4195.
(67) Pecchia, A.; Salvucci, L.; Penazzi, G.; Di Carlo, A. Non-Equilibrium Green's Functions in Density Functional Tight Binding: Method and Applications. *New J. Phys.* **2008**, *10*, 065022.
(68) Choi, H. J.; Ihm, J. *Ab initio* Pseudopotential Method for the Calculation of Conductance in Quantum Wires. *Phys. Rev. B: Condens. Matter Mater. Phys.* **1999**, *59*, 2267−2275.
(69) Giannozzi, P.; Baroni, S.; Bonini, N.; Calandra, M.; Car, R.; Cavazzoni, C.; Ceresoli, D.; Chiarotti, G. L.; Cococcioni, M.; Dabo, I.; et al. QUANTUM ESPRESSO: A Modular and Open-source Software Project for Quantum Simulations of Materials. *J. Phys.: Condens. Matter* **2009**, *21*, 395502.
(70) Sclauzero, G.; Dal Corso, A.; Smogunov, A. Interaction of CO with an Au Monatomic Chain at Different Strains: Electronic Structure and Ballistic Transport. *Phys. Rev. B: Condens. Matter Mater. Phys.* **2012**, *85*, 165411.
(71) Lücke, A.; Schmidt, W. G.; Rauls, E.; Ortmann, F.; Gerstmann, U. Influence of Structural Defects and Oxidation onto Hole Conductivity in P3HT. *J. Phys. Chem. B* **2015**, *119*, 6481−6491.
(72) Bergfield, J. P.; Solomon, G. C.; Stafford, C. A.; Ratner, M. A. Novel Quantum Interference Effects in Transport through Molecular Radicals. *Nano Lett.* **2011**, *11*, 2759−2764.
(73) Bergfield, J. P.; Stafford, C. A. Many-body Theory of Electronic Transport in Single-Molecule Heterojunctions. *Phys. Rev. B: Condens. Matter Mater. Phys.* **2009**, *79*, 245125.
(74) Hedin, L. New Method for Calculating the One-Particle Green's Function with Application to the Electron-Gas Problem. *Phys. Rev.* **1965**, *139*, A796.
(75) Thygesen, K. S.; Rubio, A. Conserving *GW* Scheme for Nonequilibrium Quantum Transport in Molecular Contacts. *Phys. Rev. B: Condens. Matter Mater. Phys.* **2008**, *77*, 115333.
(76) Mowbray, D. J.; Jones, G.; Thygesen, K. S. Influence of Functional Groups on Charge Transport in Molecular Junctions. *J. Chem. Phys.* **2008**, *128*, 111103.
(77) Garcia-Lastra, J. M.; Rostgaard, C.; Rubio, A.; Thygesen, K. S. Polarization-Induced Renormalization of Molecular Levels at Metallic and Semiconducting Surfaces. *Phys. Rev. B: Condens. Matter Mater. Phys.* **2009**, *80*, 245427.
(78) Quek, S. Y.; Choi, H. J.; Louie, S. G.; Neaton, J. B. Length Dependence of Conductance in Aromatic Single-Molecule Junctions. *Nano Lett.* **2009**, *9*, 3949−3953.
(79) Kaasbjerg, K.; Thygesen, K. S. Benchmarking GW against Exact Diagonalization for Semiempirical Models. *Phys. Rev. B: Condens. Matter Mater. Phys.* **2010**, *81*, 085102.

DOI: 10.1021/acs.jpclett.6b02989
J. Phys. Chem. Lett. 2017, 8, 727−732